Oncogene. Author manuscript; available in PMC 2018 February 06.

Published in final edited form as:

Oncogene. 2018 February 01; 37(5): 651–662. doi:10.1038/onc.2017.372.

Hypoxia activates cadherin-22 synthesis via eIF4E2 to drive cancer cell migration, invasion and adhesion

NJ Kelly[1], **JFA Varga**[1], **EJ Specker**[1], **CM Romeo**[1], **BL Coomber**[2], and **J Uniacke**[1]

[1]Department of Molecular and Cellular Biology, University of Guelph, Guelph, Ontario, Canada

[2]Department of Biomedical Sciences, Ontario Veterinary College, University of Guelph, Guelph, Ontario, Canada

Abstract

Hypoxia is a driver of cell movement in processes such as development and tumor progression. The cellular response to hypoxia involves a transcriptional program mediated by hypoxia-inducible factors, but translational control has emerged as a significant contributor. In this study, we demonstrate that a cell–cell adhesion molecule, cadherin-22, is upregulated in hypoxia via mTORC1-independent translational control by the initiation factor eIF4E2. We identify new functions of cadherin-22 as a hypoxia-specific cell-surface molecule involved in cancer cell migration, invasion and adhesion. Silencing eIF4E2 or cadherin-22 significantly impaired MDA-MB-231 breast carcinoma and U87MG glioblastoma cell migration and invasion only in hypoxia, while reintroduction of the respective exogenous gene restored the normal phenotype. Cadherin-22 was evenly distributed throughout spheroids and required for their formation and support of a hypoxic core. Conversely, E-cadherin translation was repressed by hypoxia and only expressed in the oxygenated cells of U87MG spheroids. Furthermore, immunofluorescence on paraffin-embedded human tissue from 40 glioma and 40 invasive ductal breast carcinoma patient specimens revealed that cadherin-22 expression colocalized with areas of hypoxia and significantly correlated with tumor grade and progression-free survival or stage and tumor size, respectively. This study broadens our understanding of tumor progression and metastasis by highlighting cadherin-22 as a potential new target of cancer therapy to disable hypoxic cancer cell motility and adhesion.

INTRODUCTION

The major mode of mRNA recruitment to ribosomes is via the eukaryotic initiation factor 4 F (eIF4F) at the 5′cap of mRNAs.[1] During cellular stress, mammalian target of rapamycin complex 1 (mTORC1) is impaired in its ability to phosphorylate and inhibit the 4E-binding protein (4EBP), allowing it to repress the cap-binding subunit of eIF4F, eIF4E and disrupt cap-dependent translation initiation.[2] An alternate cap-dependent mechanism is active in

Correspondence: Dr J Uniacke, Department of Molecular and Cellular Biology, University of Guelph, 50 Stone Road East, Guelph, Ontario, N1G 2W1, Canada. juniacke@uoguelph.ca.

CONFLICT OF INTEREST

The authors declare no conflict of interest.

Supplementary Information accompanies this paper on the Oncogene website (http://www.nature.com/onc)

hypoxia that utilizes the eIF4E homolog eIF4E2 in a hypoxic eIF4F complex (eIF4F^{H}).[3,4] eIF4E2 was first characterized as a translation inhibitor due to its ability to bind the 5′cap but not eIF4G, which is required to recruit ribosomes.[5] However, in hypoxia eIF4E2 interacts with eIF4G3[4] and initiates the translation of mRNAs containing 3′UTR RNA hypoxia response elements bound by hypoxia-inducible factor-2α.[3] eIF4E2 is required for tumor progression[6] and is part of a metastatic gene signature.[7] eIF4E2 is active in the lower range of physiological tissue oxygenation.[8] Hundreds of 3′UTR RNA hypoxia response element-containing transcripts have been identified including several for receptor tyrosine kinases with ties to cancer malignancy and their hypoxic synthesis via eIF4E2 is essential to tumor progression.[3,6] Another target transcript identified encodes the cell–cell adhesion molecule cadherin-22 (CDH22). Even though the *CDH22* transcript appears to contain an 3′UTR RNA hypoxia response element,[3] it has not been validated as an eIF4E2 target, nor has its contribution to hypoxia-driven processes such as tumor progression been elucidated.

Cadherins are calcium-dependent cell–cell adhesion molecules that are required for human development.[9] A classical cadherin, epithelial cadherin (E-cadherin or *CDH1*), is widely expressed in epithelial tissue. Decreased expression of E-cadherin in many human cancers is associated with de-differentiation and enhanced invasiveness.[10,11] Loss of E-cadherin in tumors can arise through mutations[12–14] or transcriptional downregulation[15–17] that can occur in a hypoxia-dependent manner.[18,19] Loss of E-cadherin is associated with a cadherin switch that causes the epithelial-to-mesenchymal transition.[10] When E-cadherin is downregulated, mesenchymal cadherins such as N-cadherin are upregulated.[20] It is an intriguing possibility that CDH22 participates in hypoxia-driven epithelial-to-mesenchymal transition during tumor progression.

CDH22 is an atypical glycophosphatidylinositol-anchored member of the cadherin superfamily that can be expressed in certain parts of the brain.[21] In a healthy animal, CDH22 is involved in morphogenesis and tissue formation in the neural and non-neural cells of the brain and neuroendocrine organs.[22] CDH22 over-expression has been associated with metastasis in colorectal carcinoma,[23] but CDH22 regulation and function has not yet been linked to hypoxia. Furthermore, hypoxia promotes increased cell adhesion and invasion,[24,25] but no hypoxia-specific cadherin has been connected to these processes.

In this study, we demonstrate that CDH22 is a hypoxia-specific cadherin that is required for cancer cells to migrate, invade and adhere to one another. We utilize two invasive cancer cell lines with contrasting E-cadherin expression: MDA-MB-231 breast carcinoma (undetectable by western blot[17]) and U87MG glioblastoma (low to moderate[26]). Blocking CDH22 with an antagonist or silencing via shRNA prevented cell migration and invasion only in hypoxia, and these phenotypes were rescued by reintroduction of exogenous CDH22. An mTORC1-independent increase in hypoxic *CDH22* mRNA translation was dependent on eIF4E2, while *CDH1* mRNA was less efficiently translated in an mTORC1-dependent manner. CDH22 had a uniform distribution and was essential for spheroids to form and maintain hypoxia. Furthermore, CDH22 expression colocalized with hypoxia in 40 glioma and 40 invasive ductal breast carcinoma patient specimens and correlated with several clinical parameters. Our data suggest that CDH22 is a hypoxia-specific cell-surface molecule that contributes to malignancy by driving cell adhesion and motility in tumor progression.

RESULTS

eIF4E2 is required for hypoxic cell migration, invasion and spheroid formation

We generated two MDA-MB-231 stable cell lines each expressing one of two independent shRNAs targeting *eIF4E2* mRNA: Knockdown (KD) 1 stably expresses shRNA targeting the 3′UTR, and KD2 the coding region (Figure 1a). *eIF4E2* transcript processing leads to several variants (Genbank) where shRNA-1 targets variant 1 (upper band of the doublet) and shRNA-2 targets all variants. These shRNAs have been used previously to show that variant 1 is essential for tumor progression.[6] Two clones of each stable cell line were utilized: KD1.1, KD1.2, KD2.1 and KD2.2. These eIF4E2-depleted MDA-MB-231 cells were significantly impaired by 57%, 85%, 58% and 70%, respectively, in their ability to close a wound in hypoxia relative to controls stably expressing non-targeting shRNA (Figure 1b). In contrast, cells cultured in normoxia displayed no significant effect (Figure 1b). Transwell migration assays demonstrated that these four eIF4E2-depleted MDA-MB-231 stable cell lines were significantly impaired, only in hypoxia, by 75%, 70%, 68%, and 61% in their ability to migrate relative to controls (Figure 1c). Next, we measured the invasive capabilities of these cells by adding a basement membrane matrix to the transwells. Two eIF4E2-depleted MDA-MB-231 stable cell lines displayed significant impairment in hypoxic, but not normoxic, invasion by 77 and 82% relative to controls (Figure 1d). To observe cell–cell adhesion, MDA-MB-231 cells were formed into spheroids where oxygen can only diffuse through approximately 10 cell layers creating a hypoxic microenvironment.[6,27] Control cells formed dense spheroids compared with the fragmented assembly of eIF4E2-depleted cells (Figure 1e). The above experiments were performed in U87MG with similar results (Supplementary Figure S1). Differences in proliferation and apoptosis between control and eIF4E2-depleted cells were not a contributing factor as there were no significant changes (Supplementary Figure S2).

Reintroduction of exogenous eIF4E2 restores the ability of hypoxic cells to migrate, invade and adhere to one another

Two stable clones each of MDA-MB-231 and U87MG eIF4E2-depleted cells were generated that express exogenous eIF4E2 (Exo1 4E2 and Exo2 4E2) (Figure 2a and Supplementary Figure 3A). The exogenous eIF4E2 escaped shRNA recognition because the shRNA recognizes the endogenous *eIF4E2* 3′UTR while the exogenous *eIF4E2* harbors the vector 3′UTR. As a control, eIF4E2-depleted cells expressing exogenous empty vector were generated. Reintroduction of eIF4E2 significantly restored the ability, relative to a control, of two MDA-MB-231 and two U87MG clones to close a wound (Figure 2b and Supplementary Figure 3B). In transwell assays, reintroduction of eIF4E2 restored the ability of hypoxic cells to migrate and invade relative to controls (Figures 2c and d and Supplementary Figures 3C and D). Exogenous eIF4E2 provided a level of hypoxic migration and invasion that was similar to that of cells stably expressing non-targeting shRNA (Figures 2b–d and Supplementary Figures S3B–D). Lastly, reintroduction of eIF4E2 restored the ability of MDA-MB-231 cells to form spheroids (Figure 2e). eIF4E2-depleted controls formed loose aggregates relative to exogenous eIF4E2-expressing cells that formed larger, dense spheres. Exogenous eIF4E2-expressing cells did not differ significantly in their proliferation or apoptosis (Supplementary Figure S2). These data demonstrate that eIF4E2 contributes

significantly to the ability of MDA-MB-231 and U87MG cells to migrate, invade and adhere to one another in hypoxia.

Hypoxia represses *CDH1* mRNA translation and activates CDH22 synthesis in an eIF4E2-dependent manner

CDH22 was identified as a potential eIF4E2 mRNA target via CLIP-seq,[3] but has yet to be validated experimentally. E-cadherin was used as a control cadherin that is transcriptionally downregulated by hypoxia leading to protein levels that are undetectable in MDA-MB-231(ref. 17) or low to moderate in U87MG.[26] We observed a decrease in E-cadherin protein in hypoxic U87MG cells (Figure 3a), but an increase in CDH22 protein in both cell lines (Figures 3a and b). Furthermore, hypoxic CDH22 protein accumulation was impaired in eIF4E2-depleted cells, while no effect was observed on E-cadherin (Figures 3a and b). Reintroduction of exogenous eIF4E2 restored hypoxic CDH22 accumulation (Figures 3c and d), but had no observable effect on E-cadherin (Figure 3c). Next, *CDH1* and *CDH22* mRNA levels were measured to determine whether their hypoxic protein reduction or accumulation, respectively, was due to altered transcript abundance. Consistent with previous reports,[18,19] *CDH1* mRNA was decreased by 63% and 34% in hypoxia relative to normoxic MDA-MB-231 and U87MG cells, respectively (Figure 3e). However, there was no significant change in *CDH22* mRNA levels (Figure 3f), suggesting that the hypoxic increase in CDH22 protein could be due to translation. Immunofluorescence of MDA-MB-231 and U87MG cells revealed CDH22 protein only in hypoxia (Figure 3g and Supplementary Figure S4). To test whether eIF4E2-dependent hypoxic CDH22 protein accumulation was due to changes in *CDH22* mRNA translation, we performed polysome fractionation analysis. In parental MDA-MB-231 and U87MG cells, *CDH1* mRNA was enriched in normoxic polysomes, but shifted to monosomes in hypoxia (Figure 4a and Supplementary Figure S5A). Conversely, *CDH22* mRNA was enriched in normoxic monosomes, but shifted into polysomes in hypoxia. *CDH22* mRNA was no longer enriched in hypoxic polysomes in eIF4E2-depleted cells when compared with controls (Figure 4b and Supplementary Figure S5B). Reintroduction of eIF4E2 restored *CDH22* mRNA association with hypoxic polysomes relative to controls (Figure 4c and Supplementary Figure S5C).

eIF4E2-dependent translation is not regulated via mTORC1 due to weak binding between eIF4E2 and 4EBP.[3,28] We tested whether *CDH22* hypoxic translation was mTORC1-dependent by incubating cells with the mTORC1 inhibitor Torin 1. When normoxic MDA-MB-231 and U87MG cells were incubated with Torin 1, *CDH1* mRNA shifted into monosomes (Figure 4d and Supplementary Figure S5D). In hypoxia, *CDH22* mRNA polysome association was unaffected by Torin 1 treatment. These data suggest that *CDH1* is translationally repressed by hypoxia and is translated in an mTORC1-dependent manner through the eIF4E-mediated machinery. Conversely, *CDH22* is translationally upregulated by hypoxia in an mTORC1-independent manner by eIF4E2.

Blocking or silencing CDH22 impairs hypoxic cell migration, invasion and spheroid formation

To test whether CDH22 is directly involved in cell migration, invasion and spheroid formation, we utilized a neutralizing antibody against the extracellular domain of CDH22.

MDA-MB-231 and U87MG cells incubated with an anti-CDH22 antibody were significantly impaired by 69% and 78%, respectively, in their ability to close a wound in hypoxia relative to controls incubated with a non-targeting IgG antibody (Figure 5a and Supplementary Figure S6A). MDA-MB-231 and U87MG cells were significantly impaired by 80% and 88%, respectively, in their ability to migrate, and by 78 and 89%, in their ability to invade a basement membrane-like matrix relative to controls (Figures 5b and c and Supplementary Figures S6B and C). The anti-CDH22 antibody had no significant effect on migration and invasion in normoxia (Figures 5a–c and Supplementary Figures S6A–C). Cells incubated with anti-CDH22 antibodies formed fragmented spheroids relative to the more dense control spheroids (Figure 5d and Supplementary Figure S6D).

The anti-CDH22 antibody detects a major band by western blot, but also a minor band that is a smaller isoform.[21] Moreover, off-target effects are unlikely because CDH22-depleted cells were not further affected in their migration and invasion when exposed to the CDH22 antibody relative to a control (Figures 5a–c). Even so, we generated stable cell lines expressing shRNA targeting the *CDH22* mRNA as another method to interfere with CDH22 function. We generated two MDA-MB-231 and two U87MG stable cell lines each expressing one of two independent shRNAs (KD3 and KD4) (Figure 6a and Supplementary Figure S7A). All CDH22-depleted cell lines were significantly impaired between 76 and 91% in their ability to close a wound generated in hypoxia, but not normoxia, relative to controls (Figure 6b and Supplementary Figure S7B). All CDH22-depleted cell lines were significantly impaired between 69 and 80% in their ability to migrate, and between 67 and 88% in their ability to invade relative to controls (Figures 6c and d and Supplementary Figures S7C and D). CDH22-depleted cells formed fragmented spheroids relative to the more dense control spheroids (Figure 6e and Supplementary Figure S7E). The fragmented CDH22-depleted spheroids were less hypoxic than control spheroids and did not display an increase in apoptosis (Figures 6f and g and Supplementary Figures 7F and G).

We performed immunofluorescence on spheroids to determine the distribution of E-cadherin (U87MG) and CDH22 (both cell lines). E-cadherin-expressing cells localized to the U87MG spheroid perimeter (Figure 7a). Spheroids are an avascular tumor model composed of a thin oxygenated shell and hypoxic interior.[6] Indeed, CDH22-expressing cells had a uniform distribution (Figures 7a–c) that colocalized with hypoxia (Figures 7b and c). Cell sorting demonstrated that E-cadherin was associated with the CA9-negative fraction of U87MG spheroids, while CDH22 with the CA9-positive hypoxic cells of both cell lines (Figure 7d). Immunofluorescence on human tumor specimens from 40 glioma (Supplementary Table S1) and 40 invasive ductal breast carcinoma cases (Supplementary Table S2) revealed that CDH22 expression significantly increased relative to normal tissue and with higher grade (glioma) or stage (breast carcinoma; Figures 7e–l). Kaplan–Meier survival curves demonstrated that low CDH22 expression significantly correlated with longer progression-free survival (PFS) in glioma patients (Figure 7m; HR = 0.3648, $P = 0.0112$), and displayed a favorable, albeit not statistically significant, progression-free survival in breast carcinoma patients (Figure 7n; HR = 0.4232, $P = 0.1040$). In a multivariate Cox proportional hazards model (adjusted for CDH22 and CA9 expression, grade or stage, and tumor size), CDH22 expression remained a statistically significant, or favorable, independent predictor of poor prognosis in glioma (hazard ratio (HR) = 0.1537, 95% confidence interval (CI) = 0.0075–

0.2999, $P = 0.0394$) and breast carcinoma (HR = 0.4551, 95% CI = 0.1816–1.2289, $P = 0.156$), respectively (Figures 7m and n). CDH22 expression also displayed a significant positive correlation with breast carcinoma tumor size (Pearson's correlation coefficient = 0.5039; Figure 7o). CDH22 colocalized with hypoxia between 82.2 ± 1.6% and 89.0 ± 1.1% regardless of glioma grade (Supplementary Table S1) or breast carcinoma stage (Supplementary Table S2). These data highlight CDH22 as a new marker for tumor hypoxia and advanced stage disease.

Reintroduction of exogenous CDH22 restores the ability of hypoxic cells to migrate, invade and adhere to one another

Two stable clones each of MDA-MB-231 and U87MG CDH22-depleted cells were generated that express exogenous CDH22 (Exo1 CDH22 and Exo2 CDH22) (Figure 8a and Supplementary Figure S8A). CDH22-depleted controls stably expressed an empty vector. Reintroduction of CDH22 significantly restored the ability, relative to a control, of two MDA-MB-231 and two U87MG clones to close a wound in hypoxia (Figure 8b and Supplementary Figure S8B). In transwell assays, exogenous CDH22 restored the ability of hypoxic cells to migrate and invade relative to CDH22-depleted controls (Figures 8c and d and Supplementary Figures S8C and D). Normoxic CDH22-depleted cells overexpressing exogenous CDH22 displayed similar increases in migration and invasion to hypoxic cells expressing endogenous CDH22 (Figures 8a–d and Supplementary Figures S8A–D). Overexpressing CDH22 in normoxic eIF4E2-depleted cells increased their migration and invasion to similar levels as hypoxic cells and restored these abilities in hypoxic eIF4E2-depleted cells (Figures 8e–h and Supplementary Figures S8E–H). Reintroduction of CDH22 restored the ability of CDH22- and eIF4E2-depleted cells to form spheroids (Figures 8i and j and Supplementary Figures S8I and J) that contained hypoxic cells (Figures 8k and l and Supplementary Figures S8K and L). Spheroid cells expressing exogenous CDH22 were not impaired in their ability to migrate or invade when presented with extracellular matrix substrates (Figures 8m and n and Supplementary Figures S8M and N). Moreover, spheroid cells overexpressing CDH22 invaded three-dimensional Matrigel significantly more than controls expressing only endogenous CDH22 (Figure 8o and Supplementary Figure S8O). No significant differences in proliferation and apoptosis were observed in these cells (Supplementary Figure S9). These data demonstrate that CDH22 contributes significantly to the ability of MDA-MB-231 and U87MG cells to migrate, invade and adhere to one another in hypoxia.

DISCUSSION

Hypoxia promotes cancer cell migration and invasion,[29–31] which are hallmarks of the disease phenotype[32] that we observed in this study. Cadherins usually participate in homophilic interactions,[9] but heterophilic adhesion complexes involving E-cadherin and N-cadherin between cancer-associated fibroblasts and cancer cells drive cooperative tumor invasion.[33] Collective cell migration is the coordinated movement of cells connected by cell–cell adhesion, and is a fundamental process in development, tissue repair, tumor invasion and metastasis.[34–36] Neoplastic cells across several cancers can display collective migration without incurring epithelial-to-mesenchymal transition.[37–39] The leading cells

produce enzymes that degrade extracellular matrix,[39] and the following cells regulate cytoskeletal dynamics via cell–cell interactions.[40] In human glioblastoma specimens, we not only observed CDH22 colocalization with hypoxia but also in areas directly adjacent (Figure 7g). This could be due to oxygen gradients emanating from necrotic foci surrounded by hypercellular regions called pseudopalisades that involve collective cell migration events.[41,42] CDH22 expression could occur in up to 5% O_2 because eIF4E2[8] and hypoxia-inducible factor-2α[43] activities are maintained at these levels. The hypoxic marker CA9 is a transcriptional target of hypoxia-inducible factor-1,[44] which is stabilized at ≤1% O_2.[43] Indeed, relative to glioblastoma, CDH22 displayed higher colocalization with hypoxia (89 ± 1.1% vs 82.2 ± 1.6%) in early stage invasive ductal breast carcinoma where pre-invasive cells are contained within the non-vascular intraductal space (Figure 7i and Supplementary Tables S1 and 2).[45] We also provide *in vitro* data supporting CDH22 as a hypoxia-specific cell–cell adhesion molecule that promotes migration and invasion in MDA-MB-231 and U87MG cells independent of E-cadherin loss. CDH22 could allow hypoxic cancer cells to adhere to one another, or to tumor-associated cells, to promote collective migration and invasion. Future studies could examine CDH22 intracellular signaling and heterotypic crosstalk by utilizing more sophisticated three-dimensional systems combining cancer and stromal cells.

Hypoxia increases cell–cell adhesion,[24] and we demonstrate that CDH22 is required for spheroid formation. Most of the spheroid volume is hypoxic (≤1% O_2) with a thin oxygenated perimeter.[6,27] Spheroids composed of cells expressing exogenous CDH22 were sturdier when handled relative to spheroids harboring only endogenous CDH22. Exogenous CDH22 is uncoupled from oxygen regulation because it contains the vector 3′UTR and not the 3′UTR RNA hypoxia response element required for its selective hypoxic expression. Consequently, exogenous CDH22 could be expressed in normoxic cells and provided a similar level of migration and invasion as hypoxia, suggesting that CDH22 is a major driver. The role of CDH22 in maintaining sphere or tumor structure and promoting collective cell migration and invasion could be interpreted as contradictory. Spheroids are formed where the only possible interactions are cell–cell. However, when spheroids expressing exogenous CDH22 were provided with extracellular matrix substrates, the cells displayed migratory or invasive capabilities. Our interpretation is that during the initial stage of spheroid or tumor formation, CDH22 is involved in maintaining the structure of the hypoxic regions and perhaps the communication between hypoxic cells. When the opportunity arises during tumor progression, such as access to extracellular matrix or a specific signaling event, CDH22 could participate in the collective invasion of hypoxic cells. Preventing hypoxic cells from not only metastasizing but adhering to one another would be an attractive strategy to shrink or fragment tumors to allow cells of the immune system, such as macrophages,[46] to better access and destroy cancer cells. CDH22 is likely not a driver of these processes in all cancers. In addition to this study, increased CDH22 expression has been linked to metastasis in colorectal carcinoma,[23] but it is decreased in metastatic melanoma.[47]

Translational control is a major target of cancer therapy.[48] Since eIF4E2 has only recently been connected to cancer progression,[6] the development of inhibitors is still in its infancy. Targeting eIF4E2 could be more specific to tumor cells by disabling hypoxic adaptation and the expression of proteins that have ties to cancer progression (EGFR, HER-2, PDGFRA,

IGF1R and now CDH22).[49,50] We show that the hypoxic translation of *CDH22* is mTORC1-independent. The mTORC1 inhibitor rapamycin was one of the first protein synthesis inhibitors used in cancer therapy, but has displayed inefficacy in the clinic.[51] We tested E-cadherin as a control cadherin with an opposite oxygen-dependent regulation to CDH22 since its hypoxic transcriptional repression has been reported.[18,19] This is the first report that *CDH1* mRNA translation efficiency is also decreased by hypoxia. Even though MDA-MB-231 cells have undetectable E-cadherin levels,[17] translation repression could be a conserved mode of regulation that can still be observed in these cells like nuclear SNAIL accumulation[52] and miRNA-mediated repression.[53] We highlight that the mTORC1-independent process of eIF4E2-dependent hypoxic translation contributes to cancer cell migration, invasion and spheroid formation.

Targeting cadherins in cancer therapy is an emerging concept.[54] The first cadherin antagonist to enter clinical trials was the ADH-1 peptide that inhibits N-cadherin. This peptide has shown promise in inhibiting melanoma and ovarian cancer.[55,56] This study broadens our understanding of tumor progression by highlighting CDH22 as a marker of advanced stage cancer and potential new therapeutic target to disable hypoxic cancer cells and prevent metastasis.

MATERIALS AND METHODS

Cell culture

MDA-MB-231 breast adenocarcinoma and U87MG glioblastoma were obtained from the American Type Culture Collection and maintained as suggested. These were tested for mycoplasma and characterized by short tandem repeat and Q-band assays. Normoxic cells were maintained in ambient O_2, 5% CO_2 and 37°C). Hypoxic cells were incubated in a HypOxystation H35 (HypOxygen, Frederick, MD, USA) at 1% O_2, 5% CO_2 and 37°C.

Constructs and short hairpin RNAs

GIPZ Lentiviral Human EIF4E2 shRNAmir (ThermoScientific, Waltham, MA, USA) was used (shRNA-1 CAGCTGAGATCACTTAATAA; shRNA-2 TGAACAGAATATCAAA). Clones were identified by shRNA and clone number. Cells stably expressing exogenous eIF4E2 were generated by transfecting cells with eIF4E2 cDNA or empty vector (Genecopoeia, Rockville, MD, USA). Psi-nU6.1 CDH22 shRNA (Genecopoeia) was used (shRNA-1 GACAGGCGACATTCATTGCC; shRNA-2 GTCGGTGATGCAGG TGATG). Non-targeting shRNA used as controls. Cells stably expressing exogenous CDH22 generated by transfecting cells with a codon-optimized CDH22 in pcDNA3.1(+) or empty vector (ThermoScientific).

Western blotting and antibodies

Standard western blotting protocols were used. Primary antibodies (1 μg/ml): CDH1 (SHE78-7; Abnova, Tapei City, Taiwan), CA9 (2D3; Novus, Littleton, CO, USA), GAPDH (D16H11; Cell Signaling Technologies, Danvers, MA, USA), active caspase-3 (ab2302; Abcam, Cambridge, UK), CDH22 (ARP49648-P050; Aviva Systems Biology, San Diego, CA, USA), eIF4E2 (GTX103977; Genetex, Irvine, CA, USA) and hypoxia-inducible

factor-2α (NB100-122; Novus). Membranes were probed with 0.1 μg/ml horseradish peroxidase-conjugated secondary antibodies.

Scratch wound assay

Cells were grown as monolayers in six-well dishes. For hypoxia, cells and media were pre-conditioned at 1% O_2 for 24 h. Wounds were generated using a micropipette tip. Images taken at 0 and 12 h (U87MG) or 16 h (MDA-MB-231). For quantification, wounds were measured. When applicable, 0.4 μg/ml control IgG (sc-2027; Santa Cruz, Dallas, TX, USA) or anti-CDH22 antibodies (Aviva Systems Biology) were added.

Migration and invasion assays

Transwell inserts (Corning, Corning, NY, USA) for 24-well plates (6.5 mm diameters and 8 μm pores) were used. Inserts were coated with 20 μg/ml fibronectin (Corning) and incubated at 4 °C for 24 h. Cells (4×10^5) seeded in serum-free Dulbecco's modified Eagle's medium in the upper chamber, and Dulbecco's modified Eagle's medium (10% fetal bovine serum) placed in lower chamber. After 16 h (MDA-MB-231) or 12 h (U87MG), cells that did not migrate were removed with a cotton swab and inserts fixed and stained with 0.15% crystal violet. For quantification, cells were counted. When applicable, 0.4 μg/ml control IgG or anti-CDH22 antibodies were added to the upper chamber. For invasion assays, Biocoat Growth Factor Reduced Matrigel Invasion Chambers (Corning) were used. For spheroid migration, 4-day-old spheroids were placed in cell culture-treated 24-well dishes and migration measured after 16 h. Three-dimensional spheroid invasion was performed as previously described.[57]

Spheroid formation, immunofluorescence and cell sorting

Cells (1×10^5) seeded in 24-well dishes pre-coated with 1% low melting agarose. MDA-MB-231 cells required 1 × Cultrex 10 × Spheroid Formation ECM (Trevigen, Gaithersburg, MD, USA). Plates were swirled for 30 min. When applicable, 0.4 μg/ml control IgG or anti-CDH22 antibodies were added. Spheroids collected after 96 h and lysed in 4% sodium dodecyl sulfate in phosphate-buffered saline for western blot. Spheroids for immunofluorescence were fixed in 4% para-formaldehyde, embedded in TissuePlus O.C.T. (ThermoScientific). Frozen spheroids were cut into 10 μm sections onto poly-L-lysine slides using the Leica CM 1860 Cryostat (Wetzlar, Germany). Slides were quenched using 0.15 M glycine and incubated for 30 min at 75 °C in antigen retrieval solution (10 mM sodium citrate and 0.05% Tween 20). Slides were stained with 3 μg/ml anti-CDH22 (NBP1-88300; Novus), anti-CDH1 (Abnova) or anti-CA9 (Novus) antibodies and 10 μg/ml Alexa Fluor 488 (4412 S; Cell Signaling Technologies), Alexa Fluor 555 (A21422; ThermoScientific) and Hoechst. Images acquired on a Nikon Eclipse Ti Microscope (Minato, Japan). Cell sorting was performed on the basis of anti-CA9 (Novus) antibody positivity as previously described[58] with a FACSAria IIu (BD Biosciences, San Jose, CA, USA).

Human tumor specimens

Human tumor specimens consisting of 5 μm paraffin sections from formalin-fixed tissue collected at surgical resection were obtained from the Brain Tumour Tissue Bank in London,

Ontario (40 glioma cases and 10 adjacent normal brain tissue) or from the Ontario Tumour Bank (40 invasive ductal breast carcinoma cases and 10 adjacent normal breast tissue), which are supported by the Brain Tumour Foundation of Canada and the Ontario Institute for Cancer Research through funding provided by the Government of Ontario, respectively. Glioma specimens were classified according to WHO criteria (Supplementary Table S1). Specimens were obtained from the tumor center and did not contain extensive hemorrhagic, necrotic or fibrous tissue. Staging of breast cancer samples was performed via the TNM system (Supplementary Table S2). Xylene and serial dilution of ethanol were used to remove paraffin and antigen retrieval was performed at 85°C for 30 min (10 mM Tris Base, 1 mM EDTA, 0.05% Tween 20, pH 9.0). Slides were washed with TBS+0.025% Triton-X-100 and blocked in 10% goat serum with 1% bovine serum albumin in TBS for 2 h at room temperature. Anti-CDH22 (Novus) and CA9 antibodies (Novus) were applied at 10 μg/ml overnight at 4 °C. Primary antibody was omitted for negative controls. Sections were counterstained with 10 μg/ml Alexa Fluor 555 (Life Technologies, Carlsbad, CA, USA), Alexa Fluor 488 (Cell Signaling Technologies) and Hoechst. Slides were mounted with ProLong Gold (ThermoScientific). CA9 and CDH22 expression was quantified using ImageJ (NIH, Bethesda, MA, USA).[59] Pixels were considered positive for the marker if the signal intensity was greater than the set threshold (2.5-fold greater than background). Colocalization analyses performed using Coloc2 in the ImageJ Fiji plugin to calculate fractional overlap between CA9 and CDH22 using Manders' Colocalization Coefficients and the Costes method for estimating thresholds above background.[60] Full and informed patient consent was obtained, and the project approved by the University of Guelph Research Ethics Board Committee, Ontario Institute for Cancer Research Ethics Committee and Brain Tumour Tissue Bank Ethics Committee.

Bromodeoxyuridine and active caspase-3 assays

Cells were seeded and incubated for 48 h in Dulbecco's modified Eagle's medium (10% fetal bovine serum). For measuring proliferation, hypoxic cells were incubated in 1% O_2 for 24 h prior to the addition of 0.1% 5-bromo-2′deoxyuridine (BrdU; Roche, Basel, Switzerland) for 1 h, fixed with 70% ethanol in 50 mM glycine (pH 2.0) for 30 min, blocked in 5% bovine serum albumin for 1 h, and stained with 10 μg/ml anti-BrdU antibody according to the manufacturer's protocol. Coverslips were counterstained with 2 μg/ml Alexa Fluor 555 and Hoechst. The BrdU labeling index was defined by the ratio of BrdU-positive nuclei to total nuclei. For measuring activation of apoptosis, cells were fixed in cold methanol for 10 min followed by acetone for 1 min. Cells were blocked for 2 h in 5% bovine serum albumin, and incubated with 3 μg/ml anti-active caspase-3 antibody (Abcam) followed by 10 μg/ml Alexa555 antibody and Hoechst.

Polysome profiling and PCR

Polysome profiling, RNA extraction and PCR were performed as previously described.[8] Primer sequences: CDH1 forward: 5′-TGCCCAGAAAATGAAAAAGG -3′; CDH1 reverse: 5′-GTGTATGTGGCAATGCGTTC-3′; CDH22 forward: 5′-TGTAT GCGAGGATGCCAAGC-3′; CDH22 reverse: 5′-AAATGAGGGTTGCTGGGAGC-3′; RPLPO forward: 5′-AACATCTCCCCCTTCTCC-3′; and RPLPO reverse: 5′-CCAGGAAGCGAGAATGC-3′.

Statistical analysis

For patient samples, cases were dichotomized based on median %CDH22 expression. Progression-free survival was defined as days post-surgical resection of tumor until recurrence (glioma) and/or disease spread (breast carcinoma). Kaplan–Meier method (univariate) was used to construct survival curves and log-rank tests to assess differences between groups. Multivariate Cox analysis was performed and the adjusted hazard ratio was calculated based on Cox models. Experimental data were tested using unpaired two-tailed Student's *t*-test when only two means were compared, or a one-way ANOVA followed by Tukey's HSD test when three or more means were compared. $P<0.05$ was considered statistically significant.

Supplementary Material

Refer to Web version on PubMed Central for supplementary material.

Acknowledgments

We thank Terry Van Raay for the use of his microscope, Scott Ryan and John Vessey for the use of their cryostat, and Marc Coppolino for technical advice and reagents. This work was funded by grants from the Canadian Institutes of Health Research (PJT 152925) and the Cancer Research Society to JU.

References

1. Gebauer F, Hentze MW. Molecular mechanisms of translational control. Nat Rev Mol Cell Biol. 2004; 5:827–835. [PubMed: 15459663]
2. Lin TA, Kong X, Haystead TA, Pause A, Belsham G, Sonenberg N, et al. PHAS-I as a link between mitogen-activated protein kinase and translation initiation. Science. 1994; 266:653–656. [PubMed: 7939721]
3. Uniacke J, Holterman CE, Lachance G, Franovic A, Jacob MD, Fabian MR, et al. An oxygen-regulated switch in the protein synthesis machinery. Nature. 2012; 486:126–129. [PubMed: 22678294]
4. Ho JJ, Wang M, Audas TE, Kwon D, Carlsson SK, Timpano S, et al. Systemic reprogramming of translation efficiencies on oxygen stimulus. Cell Rep. 2016; 14:1293–1300. [PubMed: 26854219]
5. Rom E, Kim HC, Gingras AC, Marcotrigiano J, Favre D, Olsen H, et al. Cloning and characterization of 4EHP, a novel mammalian eIF4E-related cap-binding protein. J Biol Chem. 1998; 273:13104–13109. [PubMed: 9582349]
6. Uniacke J, Perera JK, Lachance G, Francisco CB, Lee S. Cancer cells exploit eIF4E2-directed synthesis of hypoxia response proteins to drive tumor progression. Cancer Res. 2014; 74:1379–1389. [PubMed: 24408918]
7. Ramaswamy S, Ross KN, Lander ES, Golub TR. A molecular signature of metastasis in primary solid tumors. Nat Genet. 2003; 33:49–54. [PubMed: 12469122]
8. Timpano S, Uniacke J. Human cells cultured under physiological oxygen utilize two cap-binding proteins to recruit distinct mRNAs for translation. J Biol Chem. 2016; 291:10772–10782. [PubMed: 27002144]
9. Gumbiner BM. Cell adhesion: the molecular basis of tissue architecture and morphogenesis. Cell. 1996; 84:345–357. [PubMed: 8608588]
10. Christofori G, Semb H. The role of the cell-adhesion molecule E-cadherin as a tumour-suppressor gene. Trends Biochem Sci. 1999; 24:73–76. [PubMed: 10098402]
11. Jeanes A, Gottardi CJ, Yap AS. Cadherins and cancer: how does cadherin dysfunction promote tumor progression? Oncogene. 2008; 27:6920–6929. [PubMed: 19029934]

12. De Leeuw WJ, Berx G, Vos CB, Peterse JL, Van de Vijver MJ, Litvinov S, et al. Simultaneous loss of E-cadherin and catenins in invasive lobular breast cancer and lobular carcinoma in situ. J Pathol. 1997; 183:404–411. [PubMed: 9496256]
13. Guilford P, Hopkins J, Harraway J, McLeod M, McLeod N, Harawira P, et al. E-cadherin germline mutations in familial gastric cancer. Nature. 1998; 392:402–405. [PubMed: 9537325]
14. Sawada K, Mitra AK, Radjabi AR, Bhaskar V, Kistner EO, Tretiakova M, et al. Loss of E-cadherin promotes ovarian cancer metastasis via alpha 5-integrin, which is a therapeutic target. Cancer Res. 2008; 68:2329–2339. [PubMed: 18381440]
15. Batlle E, Sancho E, Franci C, Dominguez D, Monfar M, Baulida J, et al. The transcription factor snail is a repressor of E-cadherin gene expression in epithelial tumour cells. Nat Cell Biol. 2000; 2:84–89. [PubMed: 10655587]
16. Comijn J, Berx G, Vermassen P, Verschueren K, van Grunsven L, Bruyneel E, et al. The two-handed E box binding zinc finger protein SIP1 downregulates E-cadherin and induces invasion. Mol Cell. 2001; 7:1267–1278. [PubMed: 11430829]
17. Lombaerts M, van Wezel T, Philippo K, Dierssen JW, Zimmerman RM, Oosting J, et al. E-cadherin transcriptional downregulation by promoter methylation but not mutation is related to epithelial-to-mesenchymal transition in breast cancer cell lines. Br J Cancer. 2006; 94:661–671. [PubMed: 16495925]
18. Imai T, Horiuchi A, Wang C, Oka K, Ohira S, Nikaido T, et al. Hypoxia attenuates the expression of E-cadherin via up-regulation of SNAIL in ovarian carcinoma cells. Am J Pathol. 2003; 163:1437–1447. [PubMed: 14507651]
19. Krishnamachary B, Zagzag D, Nagasawa H, Rainey K, Okuyama H, Baek JH, et al. Hypoxia-inducible factor-1-dependent repression of E-cadherin in von Hippel-Lindau tumor suppressor-null renal cell carcinoma mediated by TCF3, ZFHX1A, and ZFHX1B. Cancer Res. 2006; 66:2725–2731. [PubMed: 16510593]
20. Wheelock MJ, Shintani Y, Maeda M, Fukumoto Y, Johnson KR. Cadherin switching. J Cell Sci. 2008; 121(Pt 6):727–735. [PubMed: 18322269]
21. Sugimoto K, Honda S, Yamamoto T, Ueki T, Monden M, Kaji A, et al. Molecular cloning and characterization of a newly identified member of the cadherin family, PB-cadherin. J Biol Chem. 1996; 271:11548–11556. [PubMed: 8626716]
22. Wu J, Jester WF Jr, Laslett AL, Meinhardt A, Orth JM. Expression of a novel factor, short-type PB-cadherin, in Sertoli cells and spermatogenic stem cells of the neonatal rat testis. J Endocrinol. 2003; 176:381–391. [PubMed: 12630923]
23. Zhou J, Li J, Chen J, Liu Y, Gao W, Ding Y. Over-expression of CDH22 is associated with tumor progression in colorectal cancer. Tumour Biol. 2009; 30:130–140. [PubMed: 19546606]
24. Indovina P, Rainaldi G, Santini MT. Hypoxia increases adhesion and spreading of MG-63 three-dimensional tumor spheroids. Anticancer Res. 2008; 28(2A):1013–1022. [PubMed: 18507049]
25. Zhong H, De Marzo AM, Laughner E, Lim M, Hilton DA, Zagzag D, et al. Over-expression of hypoxia-inducible factor 1alpha in common human cancers and their metastases. Cancer Res. 1999; 59:5830–5835. [PubMed: 10582706]
26. Zhu Y, Yang P, Wang Q, Hu J, Xue J, Li G, et al. The effect of CXCR4 silencing on epithelial-mesenchymal transition related genes in glioma U87 cells. Anat Rec (Hoboken). 2013; 296:1850–1856. [PubMed: 24150861]
27. Franko AJ, Sutherland RM. Oxygen diffusion distance and development of necrosis in multicell spheroids. Radiat Res. 1979; 79:439–453. [PubMed: 482606]
28. Tee AR, Tee JA, Blenis J. Characterizing the interaction of the mammalian eIF4E-related protein 4EHP with 4E-BP1. FEBS Lett. 2004; 564:58–62. [PubMed: 15094042]
29. Chen J, Imanaka N, Chen J, Griffin JD. Hypoxia potentiates Notch signaling in breast cancer leading to decreased E-cadherin expression and increased cell migration and invasion. Br J Cancer. 2010; 102:351–360. [PubMed: 20010940]
30. Krishnamachary B, Berg-Dixon S, Kelly B, Agani F, Feldser D, Ferreira G, et al. Regulation of colon carcinoma cell invasion by hypoxia-inducible factor 1. Cancer Res. 2003; 63:1138–1143. [PubMed: 12615733]

31. Zagzag D, Lukyanov Y, Lan L, Ali MA, Esencay M, Mendez O, et al. Hypoxia-inducible factor 1 and VEGF upregulate CXCR4 in glioblastoma: implications for angiogenesis and glioma cell invasion. Lab Invest. 2006; 86:1221–1232. [PubMed: 17075581]
32. Hanahan D, Weinberg RA. Hallmarks of cancer: the next generation. Cell. 2011; 144:646–674. [PubMed: 21376230]
33. Labernadie A, Kato T, Brugues A, Serra-Picamal X, Derzsi S, Arwert E, et al. A mechanically active heterotypic E-cadherin/N-cadherin adhesion enables fibro-blasts to drive cancer cell invasion. Nat Cell Biol. 2017; 19:224–237. [PubMed: 28218910]
34. Friedl P, Gilmour D. Collective cell migration in morphogenesis, regeneration and cancer. Nat Rev Mol Cell Biol. 2009; 10:445–457. [PubMed: 19546857]
35. Friedl P, Locker J, Sahai E, Segall JE. Classifying collective cancer cell invasion. Nat Cell Biol. 2012; 14:777–783. [PubMed: 22854810]
36. Rorth P. Collective cell migration. Annu Rev Cell Dev Biol. 2009; 25:407–429. [PubMed: 19575657]
37. Giampieri S, Manning C, Hooper S, Jones L, Hill CS, Sahai E. Localized and reversible TGFbeta signalling switches breast cancer cells from cohesive to single cell motility. Nat Cell Biol. 2009; 11:1287–1296. [PubMed: 19838175]
38. Kitamura T, Kometani K, Hashida H, Matsunaga A, Miyoshi H, Hosogi H, et al. SMAD4-deficient intestinal tumors recruit CCR1+ myeloid cells that promote invasion. Nat Genet. 2007; 39:467–475. [PubMed: 17369830]
39. Wolf K, Wu YI, Liu Y, Geiger J, Tam E, Overall C, et al. Multi-step pericellular proteolysis controls the transition from individual to collective cancer cell invasion. Nat Cell Biol. 2007; 9:893–904. [PubMed: 17618273]
40. Hidalgo-Carcedo C, Hooper S, Chaudhry SI, Williamson P, Harrington K, Leitinger B, et al. Collective cell migration requires suppression of actomyosin at cell-cell contacts mediated by DDR1 and the cell polarity regulators Par3 and Par6. Nat Cell Biol. 2011; 13:49–58. [PubMed: 21170030]
41. Martinez-Gonzalez A, Calvo GF, Perez Romasanta LA, Perez-Garcia VM. Hypoxic cell waves around necrotic cores in glioblastoma: a biomathematical model and its therapeutic implications. Bull Math Biol. 2012; 74:2875–2896. [PubMed: 23151957]
42. Rong Y, Durden DL, Van Meir EG, Brat DJ. 'Pseudopalisading' necrosis in glio-blastoma: a familiar morphologic feature that links vascular pathology, hypoxia, and angiogenesis. J Neuropathol Exp Neurol. 2006; 65:529–539. [PubMed: 16783163]
43. Holmquist-Mengelbier L, Fredlund E, Lofstedt T, Noguera R, Navarro S, Nilsson H, et al. Recruitment of HIF-1alpha and HIF-2alpha to common target genes is differentially regulated in neuroblastoma: HIF-2alpha promotes an aggressive phenotype. Cancer Cell. 2006; 10:413–423. [PubMed: 17097563]
44. Grabmaier K, AdW MC, Verhaegh GW, Schalken JA, Oosterwijk E. Strict regulation of CAIX(G250/MN) by HIF-1alpha in clear cell renal cell carcinoma. Oncogene. 2004; 23:5624–5631. [PubMed: 15184875]
45. Espina V, Wysolmerski J, Edmiston K, Liotta LA. Attacking breast cancer at the preinvasion stage by targeting autophagy. Womens Health (Lond). 2013; 9:157–170. [PubMed: 23477322]
46. Feng M, Chen JY, Weissman-Tsukamoto R, Volkmer JP, Ho PY, McKenna KM, et al. Macrophages eat cancer cells using their own calreticulin as a guide: roles of TLR and Btk. Proc Natl Acad Sci USA. 2015; 112:2145–2150. [PubMed: 25646432]
47. Piche B, Khosravi S, Martinka M, Ho V, Li G. CDH22 expression is reduced in metastatic melanoma. Am J Cancer Res. 2011; 1:233–239. [PubMed: 21969168]
48. Bhat M, Robichaud N, Hulea L, Sonenberg N, Pelletier J, Topisirovic I. Targeting the translation machinery in cancer. Nat Rev Drug Discov. 2015; 14:261–278. [PubMed: 25743081]
49. Kuehn BM. Genomics illuminates a deadly brain cancer. JAMA. 2010; 303:925–927. [PubMed: 20215599]
50. Slamon DJ, Godolphin W, Jones LA, Holt JA, Wong SG, Keith DE, et al. Studies of the HER-2/neu proto-oncogene in human breast and ovarian cancer. Science. 1989; 244:707–712. [PubMed: 2470152]

51. Efeyan A, Sabatini DM. mTOR and cancer: many loops in one pathway. Curr Opin Cell Biol. 2010; 22:169–176. [PubMed: 19945836]
52. Lundgren K, Nordenskjold B, Landberg G. Hypoxia, Snail and incomplete epithelial-mesenchymal transition in breast cancer. Br J Cancer. 2009; 101:1769–1781. [PubMed: 19844232]
53. Hwang-Verslues WW, Chang PH, Wei PC, Yang CY, Huang CK, Kuo WH, et al. miR-495 is upregulated by E12/E47 in breast cancer stem cells, and promotes oncogenesis and hypoxia resistance via downregulation of E-cadherin and REDD1. Oncogene. 2011; 30:2463–2474. [PubMed: 21258409]
54. Blaschuk OW, Devemy E. Cadherins as novel targets for anti-cancer therapy. Eur J Pharmacol. 2009; 625:195–198. [PubMed: 19836380]
55. Beasley GM, McMahon N, Sanders G, Augustine CK, Selim MA, Peterson B, et al. A phase 1 study of systemic ADH-1 in combination with melphalan via isolated limb infusion in patients with locally advanced in-transit malignant melanoma. Cancer. 2009; 115:4766–4774. [PubMed: 19637344]
56. Perotti A, Sessa C, Mancuso A, Noberasco C, Cresta S, Locatelli A, et al. Clinical and pharmacological phase I evaluation of Exherin (ADH-1), a selective anti-N-cadherin peptide in patients with N-cadherin-expressing solid tumours. Ann Oncol. 2009; 20:741–745. [PubMed: 19190075]
57. Vinci M, Box C, Eccles SA. Three-dimensional (3D) tumor spheroid invasion assay. J Vis Exp. 2015; 99:e52686.
58. Chaudary N, Hill RP. Increased expression of metastasis-related genes in hypoxic cells sorted from cervical and lymph nodal xenograft tumors. Lab Invest. 2009; 89:587–596. [PubMed: 19308047]
59. Russell J, Carlin S, Burke SA, Wen B, Yang KM, Ling CC. Immunohistochemical detection of changes in tumor hypoxia. Int J Radiat Oncol Biol Phys. 2009; 73:1177–1186. [PubMed: 19251089]
60. Schindelin J, Arganda-Carreras I, Frise E, Kaynig V, Longair M, Pietzsch T, et al. Fiji: an open-source platform for biological-image analysis. Nat Methods. 2012; 9:676–682. [PubMed: 22743772]

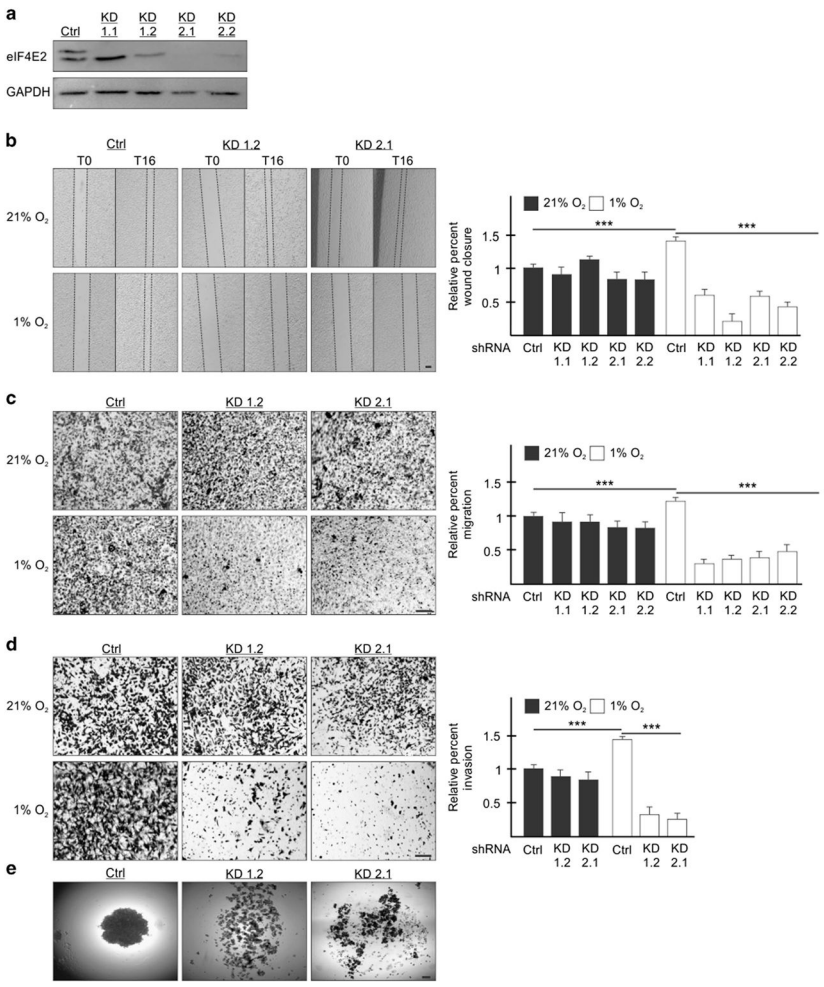

Figure 1.

eIF4E2 is required for MDA-MB-231 cell migration, invasion and spheroid formation in hypoxia. (**a**) Western blot of eIF4E2 protein levels in control (Ctrl) cells stably expressing a non-targeting shRNA or in cells stably expressing one of two shRNAs targeting *eIF4E2* mRNA: Knockdown (KD) 1 and KD2. Two clones of each stable cell line were generated: KD1.1, KD1.2, KD2.1 and KD2.2. GAPDH used as a loading control. (**b**) Control and eIF4E2 KD cells exposed to normoxia (21% O_2) or hypoxia (1% O_2) for 24 h followed by wound generation. Representative images at 0 h (T0) and 16 h (T16) after wound generation. (**c**, **d**) Transwell migration (**c**) and invasion (**d**) assays of control and eIF4E2 KD cells exposed to normoxia or hypoxia for 24 h. Representative images of transwell inserts 16 h after seeding and stained with crystal violet. (**e**) Light micrographs of spheroids composed of control cells or eIF4E2-depleted cells (KD1.2 and 2.1). Data are presented relative to normoxic Ctrl as mean ±s.e.m., $n \geq 3$, ***$P<0.001$, using a one-way ANOVA followed by Tukey's HSD test. Scale bar, 100 μm.

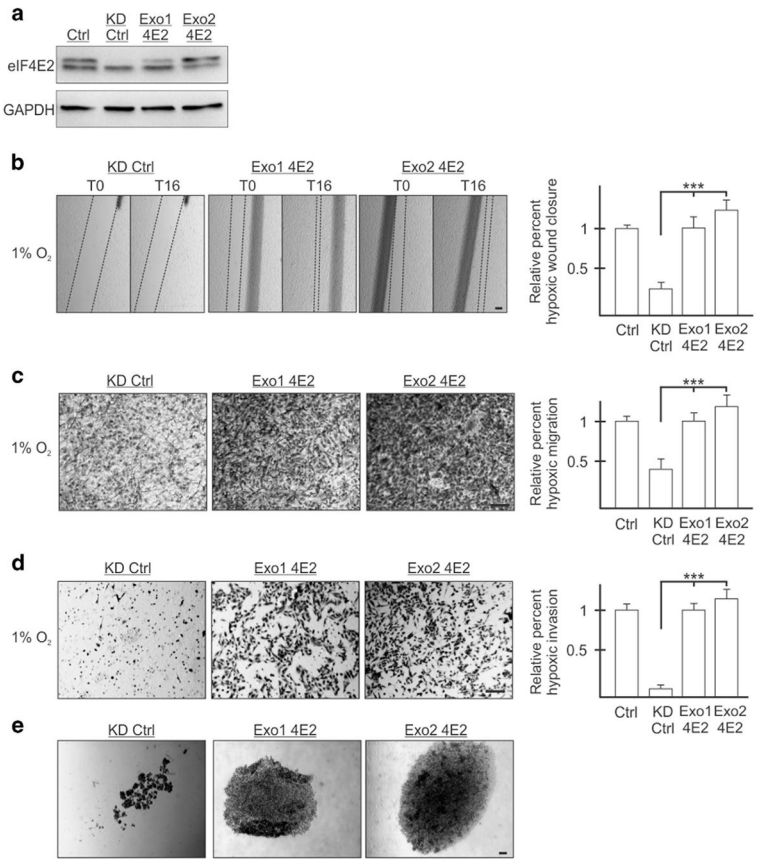

Figure 2.

Reintroduction of exogenous eIF4E2 restores the ability of MDA-MB-231 cells to migrate, invade and adhere to one another in hypoxia. (**a**) Western blot of eIF4E2 protein levels in control (Ctrl) cells stably expressing a non-targeting shRNA, eIF4E2 knockdown control (KD Ctrl) cells stably expressing shRNA targeting *eIF4E2* mRNA and an exogenous empty vector or the *eIF4E2* coding sequence (Exo1 4E2 and Exo2 4E2). GAPDH used as a loading control. (**b**) KD Ctrl, Exo1 4E2 and Exo2 4E2 cells exposed to hypoxia (1% O_2) for 24 h followed by wound generation. Representative images at 0 h (T0) and 16 h (T16) after wound generation. (**c** and **d**) Transwell migration (**c**) and invasion (**d**) assays of KD Ctrl, Exo1 4E2 and Exo2 4E2 cells exposed to hypoxia for 24 h. Representative images of transwell inserts 16 h after seeding and stained with crystal violet. (**e**) Light micrographs of spheroids composed of KD Ctrl, Exo1 4E2 and Exo2 4E2 cells. Data are presented as mean ±s.e.m., $n \geq 3$, ***$P<0.001$, using a one-way ANOVA followed by Tukey's HSD test. Scale bar, 100 μm.

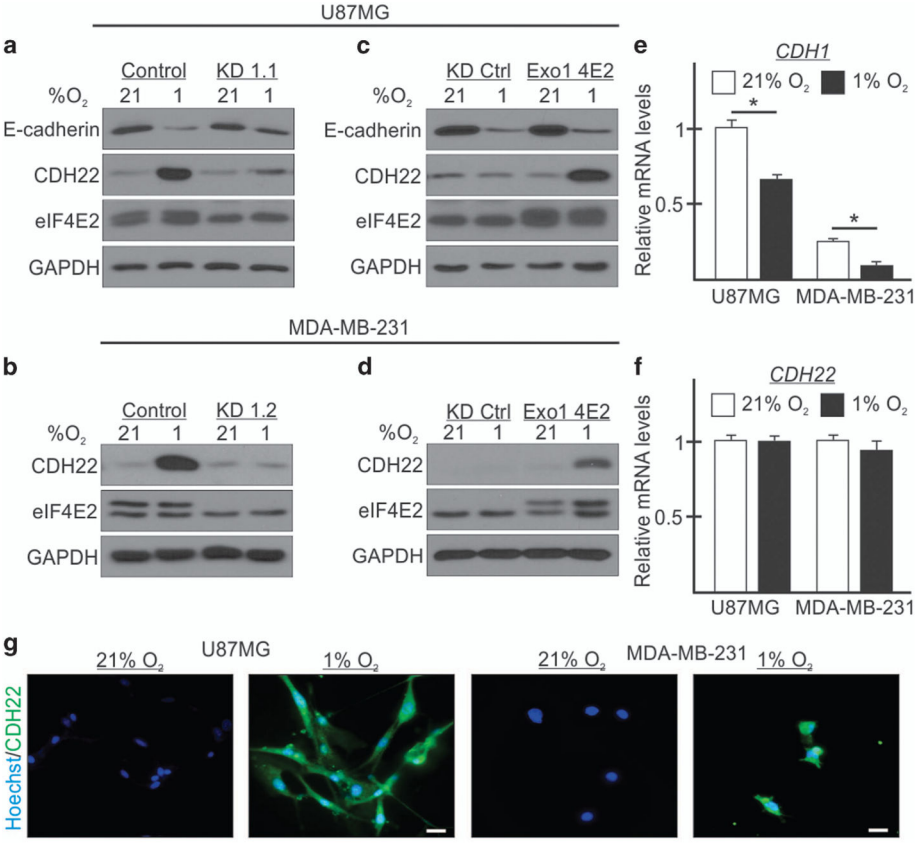

Figure 3.

Hypoxia causes CDH22 protein accumulation in an eIF4E2-dependent manner independent of its transcript abundance. (**a**–**d**) Western blot of CDH22 and eIF4E2 protein levels in normoxic (21% O_2) and hypoxic (1% O_2) U87MG (**a**, **c**) and MDA-MB-231 (**b**, **d**) control cells stably expressing a non-targeting shRNA, in cells stably expressing shRNA targeting *eIF4E2* mRNA (KD1.1 or 1.2), KD cells stably expressing an exogenous empty vector (KD Ctrl) or the *eIF4E2* coding sequence (Exo1 4E2). GAPDH used as a loading control. (**e**, **f**) *CDH1* (**e**) and *CDH22* (**f**) mRNA levels measured by quantitative reverse transcriptase–PCR in U87MG and MDA-MB-231 control cells stably expressing a non-targeting shRNA exposed to normoxia or hypoxia. Data are presented as mean ±s.e.m., n =3, *P<0.05 (Student's t-test). (**g**) Immunofluorescence of CDH22 in U87MG and MDA-MB-231 cells exposed to normoxia and hypoxia. Scale bar, 10 μm.

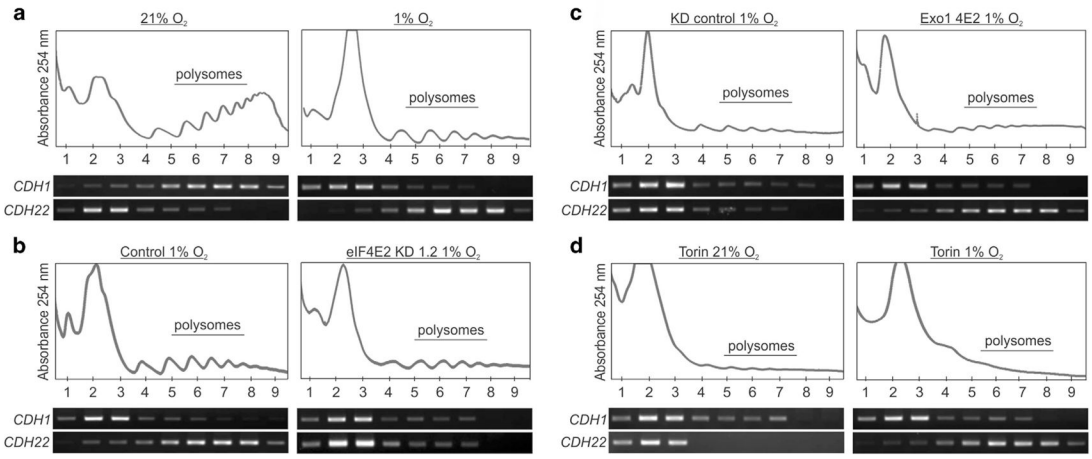

Figure 4.

Hypoxia represses *CDH1* mRNA translation and activates CDH22 synthesis in an eIF4E2-dependent manner. (**a**–**c**) The polysomal association of *CDH1* and *CDH22* mRNAs was observed by reverse transcriptase (RT)–PCR in parental (**a**), control cells stably expressing a non-targeting shRNA (**b**), or shRNA targeting *eIF4E2* mRNA (KD1.2) (**b**), KD cells stably expressing an exogenous empty vector (KD Ctrl) (**c**), or the exogenous *eIF4E2* coding sequence (Exo1 4E2) (**c**) under the indicated oxygen conditions. (**d**) The polysomal association of *CDH1* and *CDH22* mRNAs was observed by RT–PCR in parental cells exposed to normoxia or hypoxia and the mTORC1 inhibitor Torin 1 for 2 h. Images are representative of at least three biological replicates. All experiments performed in MDA-MB-231 breast carcinoma.

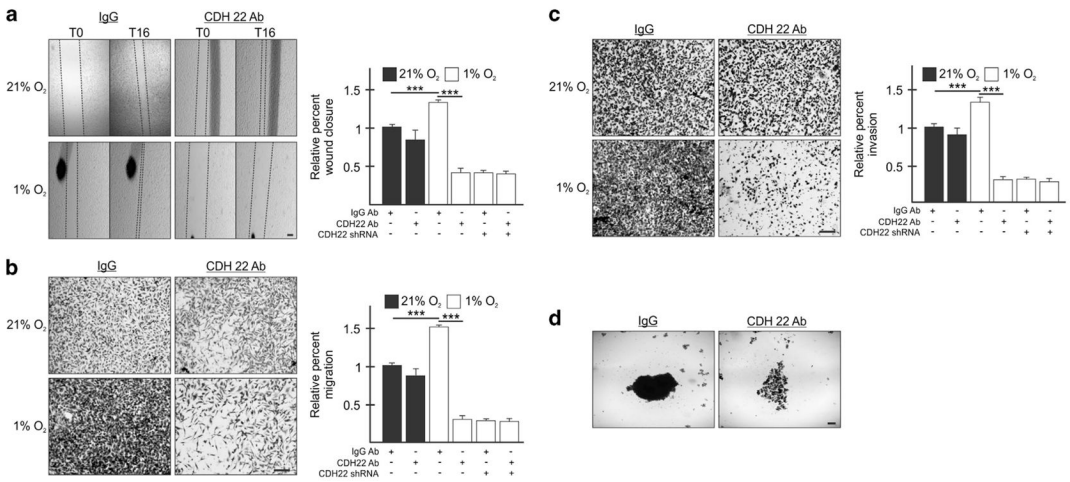

Figure 5.

Blocking CDH22 impairs hypoxic MDA-MB-231 cell migration, invasion and spheroid formation. (**a**) Parental cells or cells stably expressing shRNA targeting *CDH22* (clone KD3.1) incubated with a control non-targeting antibody (IgG) or an antibody targeting the extracellular domain of CDH22 were exposed to normoxia (21% O_2) or hypoxia (1% O_2) for 24 h followed by wound generation. Representative images at 0 h (T0) and 16 h (T16) after wound generation. (**b**, **c**) Transwell migration (**b**) and invasion (**c**) assays of parental cells or cells stably expressing shRNA targeting *CDH22* incubated with control or anti-CDH22 antibodies and exposed to normoxia or hypoxia for 24 h. Representative images of transwell inserts 16 h after seeding and stained with crystal violet. (**d**) Light micrographs of spheroids composed of parental cells incubated with control or anti-CDH22 antibodies. Data are presented relative to normoxic Ctrl as mean ±s.e.m., $n \geq 3$, ***$P<0.001$, using a one-way ANOVA followed by Tukey's HSD test. Scale bar, 100 μm.

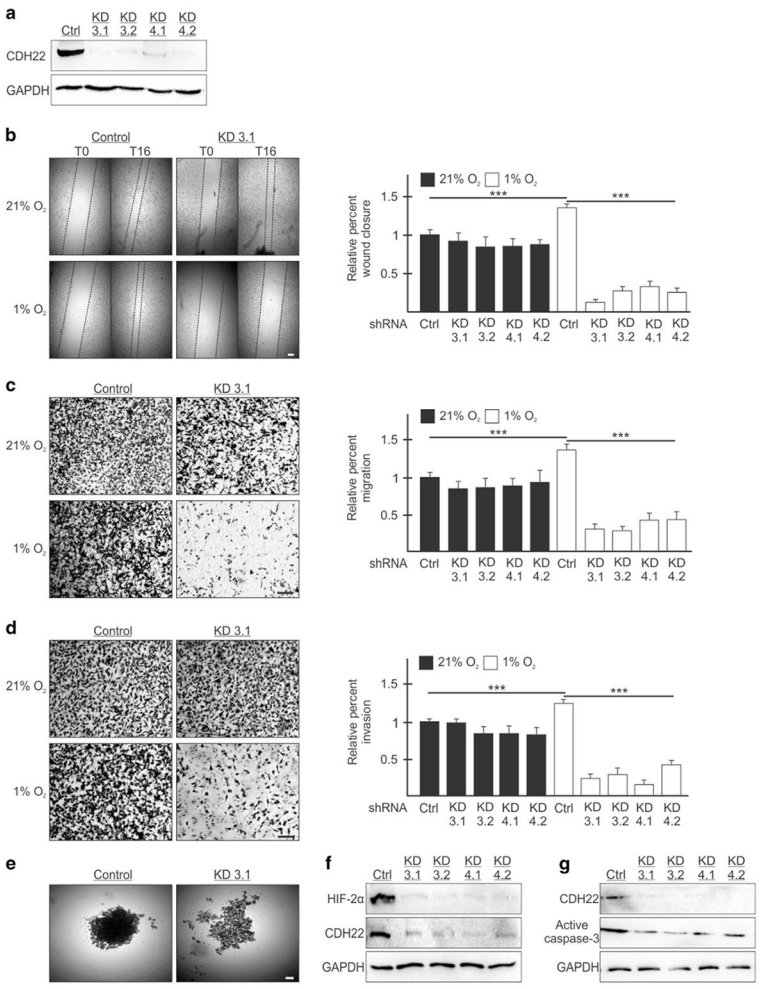

Figure 6.

Silencing CDH22 impairs hypoxic MDA-MB-231 cell migration, invasion and spheroid formation. (**a**) Western blot of CDH22 hypoxic protein levels in control (Ctrl) cells stably expressing a non-targeting shRNA or in cells stably expressing one of two shRNAs targeting *CDH22* mRNA: Knockdown (KD) 3 and KD4. Two clones of each were generated: KD3.1, KD3.2, KD4.1 and KD4.2. GAPDH used as a loading control. (**b**) Control and CDH22 KD cells exposed to normoxia (21% O_2) or hypoxia (1% O_2) for 24 h followed by wound generation. Representative images at 0 h (T0) and 16 h (T16) after wound generation. (**c**, **d**) Transwell migration (**c**) and invasion (**d**) assays of control and CDH22 KD cells exposed to normoxia or hypoxia for 24 h. Representative images of transwell inserts 16 h after seeding and stained with crystal violet. (**e**) Light micrographs of spheroids composed of control cells or CDH22-depleted cells (KD3.1). (**f**, **g**) Western blot of hypoxia-inducible factor-2α (**f**) and active caspase-3 (**g**) protein levels in lysates of spheroids composed of control cells or CDH22-depleted cells. Data are presented relative to normoxic Ctrl as mean ±s.e.m., $n \geq 3$, *** $P<0.001$, using a one-way ANOVA followed by Tukey's HSD test. Scale bar, 100 μm.

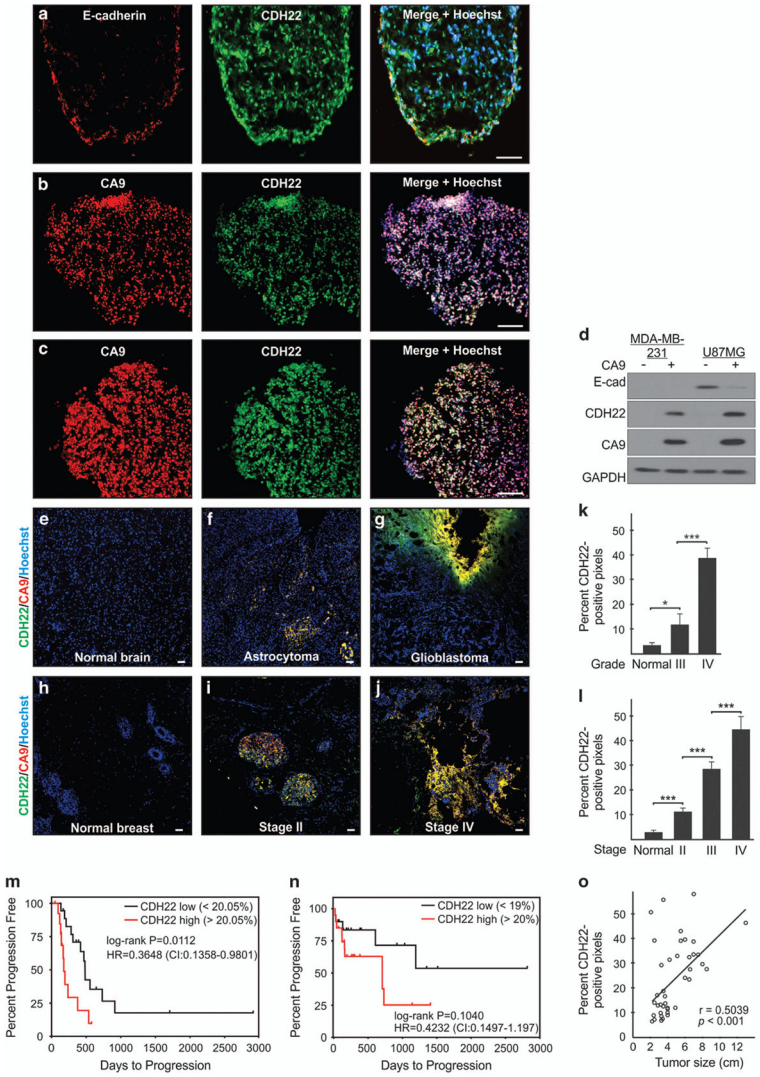

Figure 7.

CDH22 expression colocalizes with hypoxia and correlates with clinical parameters in human glioma and invasive ductal breast carcinoma. (**a**) Immunofluorescence of E-cadherin and CDH22 in U87MG spheroids. (**b**, **c**) Immunofluorescence of CDH22 and CA9 (hypoxia) in MDA-MB-231 (**b**) and U87MG (**c**) spheroids. (**d**) Sorting of CA9-positive and CA9-negative spheroid cells followed by western blot. (**e**–**j**) Immunofluorescence at × 100 magnification of CDH22 and CA9 on tissue sections from human normal brain (**e**), WHO grade III astrocytoma (**f**), WHO grade IV glioblastoma (**g**), normal breast (**h**), stage II (**i**) and stage IV breast carcinoma (**j**). Scale bar, 100 μm. Hoechst was used as a marker of cells (nuclei). (**k**) Quantification of CDH22 expression in WHO grade III glioma (n =20), WHO grade IV glioma (n =20) and normal brain tissue (n =10). (**l**) Quantification of CDH22 expression in stage II (n =19), stage III (n =11) and stage IV breast carcinoma (n =9), and normal breast tissue (n =10). *P<0.05, ***P<0.001, using a one-way ANOVA followed by Tukey's HSD test. (**m**, **n**) Kaplan–Meier plots (univariate analysis) assessing the progression-free survival of glioma (**m**; n =36, HR =0.3648, P =0.0112) and breast

carcinoma (**n**; $n = 40$, HR =0.4232, $P = 0.1040$) patients grouped into high and low CDH22 expression using the median expression as threshold. $P<0.05$ was considered statistically significant using the log-rank test. In a multivariate Cox proportional hazards model (adjusted for CDH22 and CA9 expression, grade or stage, and tumor size), CDH22 expression remained a statistically significant, or favorable, independent predictor of poor prognosis in glioma (HR =0.1537, 95% CI =0.0075–0.2999, $P = 0.0394$) and breast carcinoma (HR =0.4551, 95% CI =0.1816–1.2289, $P = 0.156$). (**o**) CDH22 expression positively correlates with breast carcinoma tumor size ($n = 40$; Pearson's correlation coefficient =0.5039, $P<0.001$). Images are representative of three biological replicates (spheroids) or 40 patient cases each of glioma and breast carcinoma summarized in Supplementary Tables S1 and S2. CI, confidence interval; HR, hazard ratio.

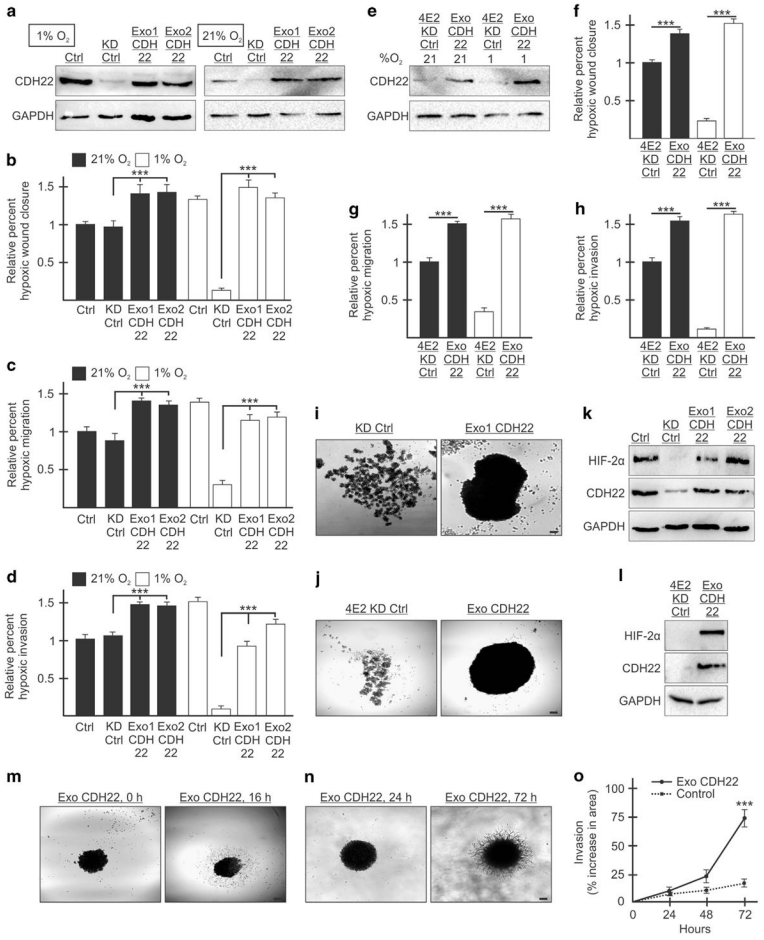

Figure 8.

Reintroduction of exogenous CDH22 restores the ability of MDA-MB-231 cells to migrate, invade and adhere to one another in hypoxia. (**a**) Western blot of control (Ctrl) cells stably expressing a non-targeting shRNA, CDH22 knockdown control (KD Ctrl) cells stably expressing shRNA targeting *CDH22* mRNA and an exogenous empty vector or *CDH22* codon-optimized coding sequence (clones Exo1 CDH22 and Exo2 CDH22) in hypoxia and normoxia. GAPDH used as a loading control. (**b**–**d**) Cells in (**a**) exposed to normoxia or hypoxia for 24 h followed by wound generation (**b**), or transwell migration (**c**) and invasion (**d**) assays. (**e**) Western blot of cells stably expressing shRNA targeting *eIF4E2* and either an empty vector (4E2KD Ctrl) or exogenous CDH22 (Exo CDH22). (**f**–**h**) Cells in (**e**) exposed to normoxia or hypoxia for 24 h followed by wound generation (**f**), or transwell migration (**g**) and invasion (**h**) assays. (**i**, **j**) Spheroids composed of CDH22-depleted (**i**) or eIF4E2-depleted (**j**) control cells expressing empty vector or exogenous CDH22. (**k**, **l**) Western blot of hypoxia-inducible factor-2α protein in lysates of spheroids from (**i**) (**k**) and **j** (**l**). (**m**, **n**) Spheroid migration assay (**m**) and three-dimensional (3D) spheroid invasion assay (**n**) of spheroids composed of cells stably expressing exogenous CDH22. (**o**) Percent increase in spheroid area (invasion) in 3D invasion assay of spheroids stably expressing exogenous CDH22 compared with controls stably expressing non-targeting shRNA. Data are presented

as mean ±s.e.m., $n \geq 3$, ***$P < 0.001$, using a one-way ANOVA followed by Tukey's HSD test. Scale bar, 100 μm.